

Chapter 7

Two- and four-pulse Ramsey spectroscopy and prospects for improved optical frequency metrology with microkelvin ^{40}Ca atoms

Our demonstration of 3-D narrow-line quenched cooling showed a reduction of Ca atom temperatures to the 10s of microkelvin range. This temperature reduction by a factor of 200 from the previous work is very promising for the reduction of velocity-dependent systematic errors for the ^{40}Ca optical frequency standard. Cold atoms will not only improve the accuracy of the system by reducing the cause of the largest systematic errors, but will make it easier to characterize and correct other shifts that have previously been masked by the larger frequency shifts caused by the velocity of the atoms. Experimental exploration of these systematics using ultracold atoms will allow us to derive a new systematic uncertainty budget for the system. This chapter outlines how ultracold ($< 10 \mu\text{K}$) atoms improve Bordé-Ramsey spectroscopy for use in frequency metrology and enable two-pulse Ramsey spectroscopy. We are in the processes of implementing new techniques for the evaluation of systematic uncertainties of our Ca clock when using ultracold atomic samples and have begun preliminary frequency and stability measurements of the system with quenched narrow-line cooled atoms. This chapter will conclude with a description of a potential direction for next-generation neutral-atom optical frequency standards, using optical lattices to trap and hold the atoms during the clock spectroscopy.

7.1 Spectroscopy with ultracold atoms

7.1.1 Four-pulse Bordé-Ramsey fringes

The application of ultracold atoms for the improvement of the ^{40}Ca optical frequency standard required a cooling scheme that would ideally have short first- and second-stage cooling cycles in order to minimize the overall measurement cycle time. We also desired the largest number of atoms to maximize S/N, as well as the coldest temperatures to best reduce velocity-dependent frequency shifts. Our experimental realization of Bordé-Ramsey fringes made with ultracold atoms took these three goals into consideration, and we found that under present experimental conditions the best compromise used 25 ms of blue cooling followed by 5 ms of red-green quenched cooling in 3-D. (Figure 7.1 shows the atom number and Bordé-Ramsey fringe size vs. cooling time.) This amount of broad-line cooling time allowed us to initially trap a large number of atoms and after 5 ms of narrow-line cooling the atom cloud had come into equilibrium (fit to a Gaussian) at a temperature of $10\ \mu\text{s}$, with 28 % transfer efficiency (5.6×10^5 of the originally trapped 2.0×10^6 atoms). With such a narrow final velocity distribution, nearly all of these ultracold atoms contribute to the Bordé-Ramsey interferometry used for frequency metrology, and the resulting lineshapes are virtually Fourier-transform-limited. In Figure 7.2(a) a single, 100-second scan taken of Bordé-Ramsey fringes at a resolution of 11.5 kHz using ultracold atoms is shown.

The contrast in this fringe pattern is 40 % and nearly all of the trapped atoms participated in the spectroscopy compared to warmer broad-line Doppler-cooled atoms where the contrast was smaller (33 %) and only 20 - 40 % of the atoms contributed to the fringe pattern. Note that the asymmetry in the fringe envelope is real: computer simulations based on the formalism developed by Bordé *et al.*[70] have shown the same asymmetric envelope and indicate that it results from atomic recoil shifts. The dotted line in Figure 7.2(a) shows the envelop of a simulated fringe pattern (generated by G.

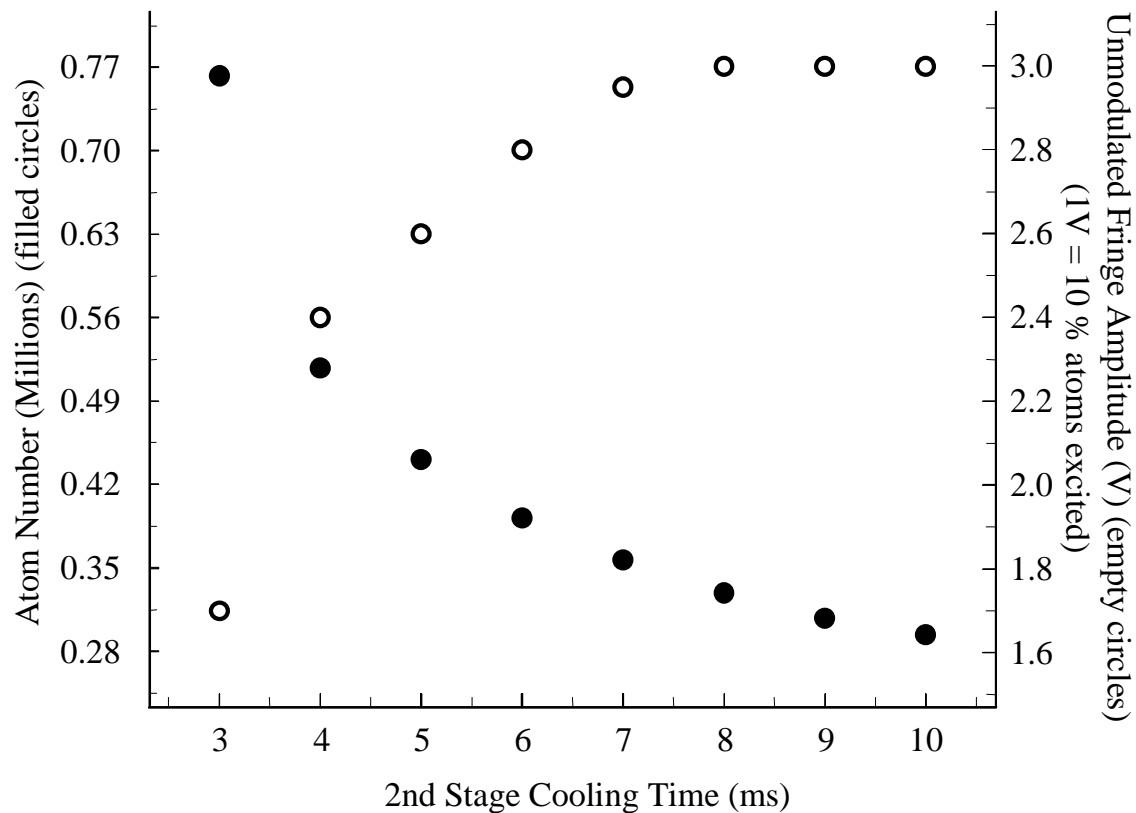


Figure 7.1: This plot shows trapped atom fluorescence (filled circles) and Bordé-Ramsey 11.5 kHz resolution fringe size (empty circles) vs. second-stage cooling time.

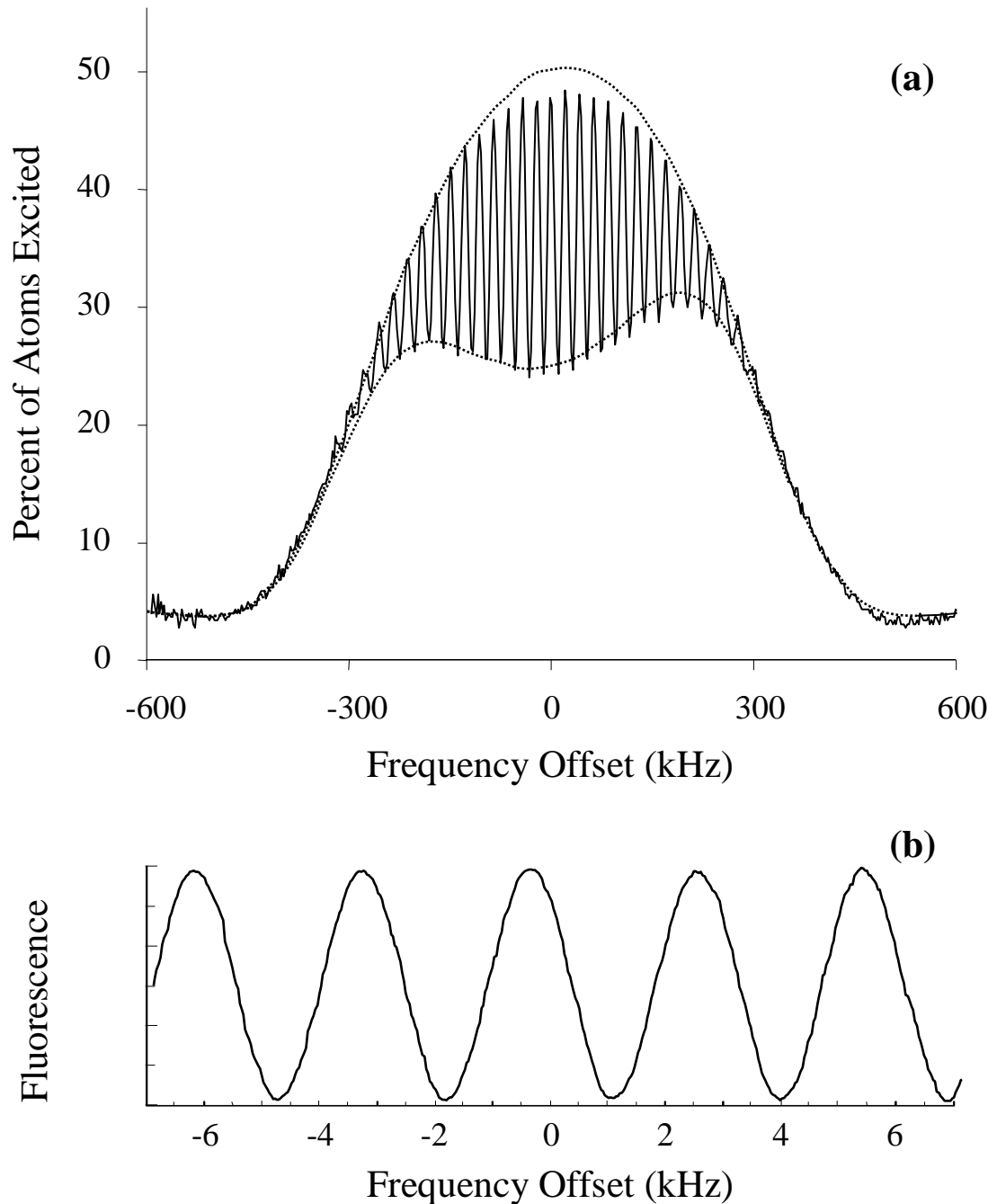


Figure 7.2: (a) Bordé-Ramsey fringe pattern based on the 657 nm clock transition with a resolution of 11.55 kHz taken after 4 ms of second-stage cooling. A single 100-second frequency sweep of the 657 nm probe laser shows high contrast, Fourier-transform-limited fringes. The asymmetric fringe envelope is a result of atomic recoil. The dotted line shows a simulation of the fringe envelope (generated by G. Wilpers) taking into consideration the experimental conditions. (b) High resolution 1.45 kHz Bordé-Ramsey fringes taken under the same cooling conditions (< 30 s averaging time.)

Wilpers), whose simulation takes many experimental parameters into account, including the temperature of the atoms, the duration and separation of the Bordé-Ramsey pulses, and the size of the atom cloud relative to the size of the spectroscopic beams. This asymmetric lineshape is quite remarkable since the recoil shift itself (23.1 kHz) is considerably smaller than the scale of the asymmetry. This asymmetry could be problematic for frequency metrology as an asymmetric baseline can offset the frequency of the central fringe. However, simulations have shown that by using high-resolution fringes (which we use for applications to frequency metrology at resolutions of ~ 1 kHz or less in order to have a more sharply defined line center), frequency shifts of the central fringe would be < 1 Hz, and can be characterized beyond this level. Figure 7.2(b) shows the central portion of a Bordé-Ramsey fringe pattern with 1.45 kHz resolution using ultracold atoms. Here the contrast is considerably larger than for millikelvin atoms.

By comparing measurements of the fringe contrast at different resolutions to the values expected from theory we can make a statement about the linewidth of our 657 nm laser system. The fringes measured in Figure 7.3 were made using atoms that had been first-stage blue cooled for 25 ms, and then second-stage red-green cooled for 4 ms, with a final temperature of ~ 15 μ K, corresponding to a $v_{rms} \sim 6$ cm/s. The resolution of these fringes range from 11.5 kHz ($T_R = 21$ μ s) to 200 Hz ($T_R = 1256$ μ s). A fit to the decay of the fringe amplitude, a solid line in Figure 7.3, gives a $1/e$ decay time of 300 μ s. If we assume only two sources for this decay, the natural linewidth Γ of the transition and the linewidth of the laser ν_l , during a time T , then the measured decay will be the product of two exponentials as given in Reference [94]:

$$e^{-2\pi\nu_l T} e^{-\Gamma T} \tag{7.1}$$

For a measured decay of 300 μ s and a lifetime of the 657 nm transition of 400 μ s, we can extrapolate a laser linewidth of 117 Hz. We have also independently measured the linewidth of the 657 nm master laser by looking at the beatnote produced between a

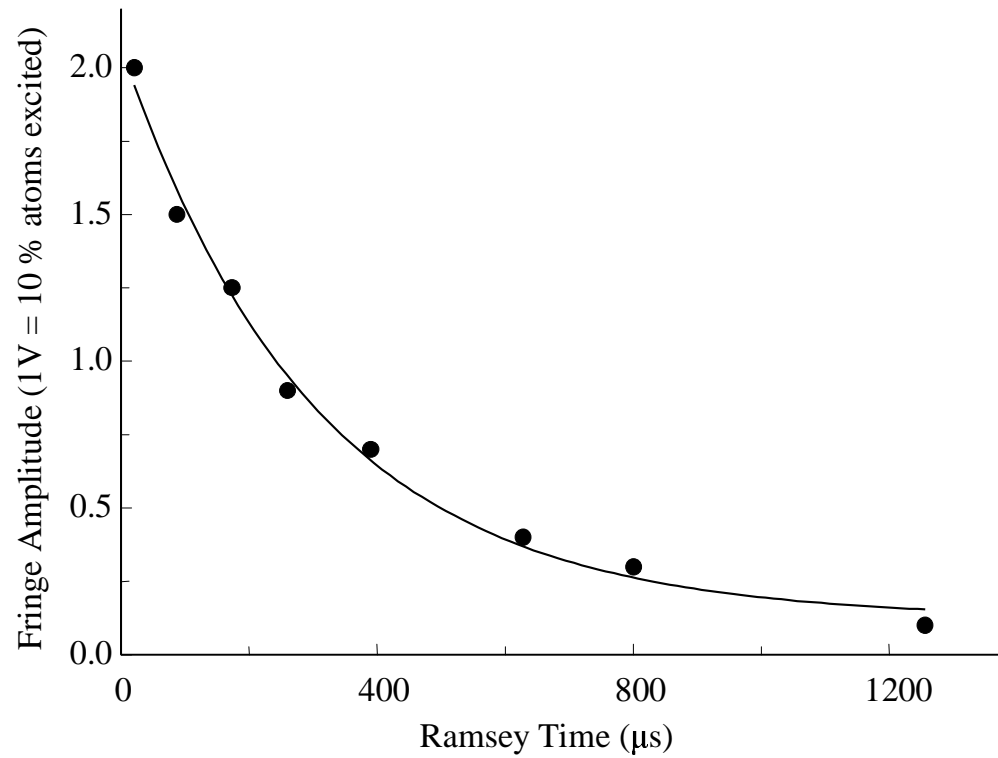


Figure 7.3: Bordé-Ramsey fringe size measured vs. fringe resolution. Fringe resolutions range from 11.5 kHz to 200 Hz. The decay constant is $300 \mu\text{s}$, leading us to believe that the linewidth of the laser producing the Bordé-Ramsey spectroscopic light is less than 117 Hz.

femtosecond laser comb tooth and the calcium light, when the comb was locked to light from the Hg^+ ion, which has a linewidth of < 7 Hz. The beatnote shown in Figure 7.4 is ~ 150 Hz wide, in good agreement with our fringe contrast decay measurement. In fact, these measurements are both upper limits, as there are other factors increasing the speed of the decay that are not taken into account in equation 7.1, and in the beatnote measurement the stability of the lock of the femtosecond comb could affect the measured width of the beatnote. We have found that the 10 m of optical fiber connecting the Ca laser and the femtosecond comb contributes $\sim 100 - 150$ Hz of spectral broadening.

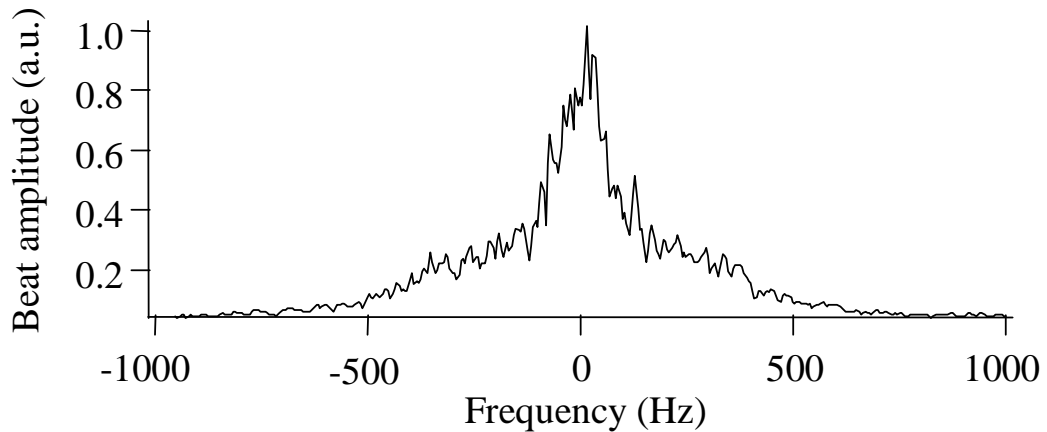


Figure 7.4: The effective beatnote between the ^{40}Ca and Hg^+ optical frequency standards achieved using a self-referenced optical frequency comb. The width is ~ 150 Hz, setting an upper limit for the laser linewidth of the Hg^+ and Ca laser systems, and the stability of the femtosecond comb and fiber noise on the calcium light. (10 Hz bandwidth)

For an accurate evaluation of the fractional frequency instability that we should be able to achieve with our Ca system we need to use a more detailed version of the theoretical limit for the stability than that given by equation 6.6, as it does not include many experimental realities that determine the S/N of the system. A more precise expression takes into consideration the fact that (i) four-pulse Bordé-Ramsey fringes only have a maximum contrast (p_0) of 0.5 and experimentally often less; (ii) we are

not necessarily working with fringe resolutions ($\Delta\nu$) as narrow as the natural linewidth of the transition, and (iii) that the length of the measurement cycle time (T_c) affects the stability. As derived in reference [72], the Allan Deviation given in equation 7.2 takes these stability-reducing factors into account when measuring the frequency on resonance, where N_0 is the number of atoms and τ is the averaging time.

$$\sigma_y(\tau) = \frac{\Delta\nu}{p_0\pi\nu_0} \sqrt{\frac{1}{2N_0}} \sqrt{\frac{T_c}{\tau}} \quad (7.2)$$

When using second-stage cooling, experimental conditions lead to a cycle time of ~ 60 ms (sampling both sides of the fringe during one cycle), $\sim 6 \times 10^5$ atoms in the ultracold cloud, and, when using a Bordé-Ramsey fringe linewidth of 11.5 kHz, a measured contrast of 40 %. In this case, equation 7.2 gives $\sigma_y(\tau) = 4.4 \times 10^{-15} \tau^{-1/2}$. For high resolution (1.45 kHz) fringes, the contrast is reduced to 27 %, but due to the smaller $\Delta\nu$, the calculated fractional frequency instability is reduced to $8 \times 10^{-16} \tau^{-1/2}$.

Preliminary measurements of the stability of the ultracold sample using Bordé-Ramsey spectroscopy and measuring the S/N of the fringes show an instability of $\sigma_y = 1-2 \times 10^{-14}$ at 1 s. Again, we believe that the discrepancy between the measured and calculated values comes from frequency noise resulting from residual environmental noise of the optical cavity. With improved contrast due to 10- μ K atoms we should be able to significantly improve the stability over that of millikelvin-atom-based clocks, but we will need to find a way to increase the trapped atom number and reduce the overall cycle time, for example, by loading faster with Zeeman-slowed atomic beam, rather than just with a slowing beam, or by physically separating the trapping and cooling region from the clock region, as is done in atomic fountains.

7.1.2 Two-pulse Ramsey fringes

I showed that additional third-stage cooling reduced temperatures even further in 1-D, with a resulting atomic velocity of < 1 cm/s or < 10 nm/ μ s, such that the atoms

were moving only a small fraction of an optical wavelength during a Bordé-Ramsey spectroscopic period. In this velocity regime we can obtain Ramsey fringe patterns using only two pulses, as is the case for microwave spectroscopy and trapped ion standards. With two-pulse Ramsey spectroscopy, the contrast of the fringes is not limited to 50 %, as in the four-pulse case, but can be 100 %, potentially improving the stability of the frequency standard by about a factor of 3, through the added contrast (times 2) and by the potential for reduction of the cycle time. Two-pulse fringe patterns for Ramsey times of 5 μs and 20 μs are shown in Figure 7.5(a) and 7.5(b), respectively. While this was the first demonstration of two-pulse optical Ramsey fringes in Ca, we note that two-pulse fringe patterns have previously been seen using the analogous transition in ultracold Sr.[95]

One can see that fringe contrast has degraded with increasing Ramsey time, from 40 % for the 5- μs Ramsey time down to 11 % for the 20- μs Ramsey time. It is only with the use of atoms with subrecoil velocities that these fringes can be clearly seen, and they remained visible even at Ramsey times of 20 μs and beyond. Not surprisingly, the fringe contrast was very sensitive to the atomic velocity: computer simulations of this process yielded velocity widths in very good agreement with our direct measurements of the velocity distributions. Due to their first-order Doppler sensitivity and reduced contrast at high resolution, these two-pulse fringes will not supersede the four-pulse variety for our immediate frequency-standard applications, but they do demonstrate the greatly increased coherence of the ultracold atomic sample.

7.2 Changes in systematics evaluation with ultracold atoms

Many of the systematic frequency shifts discussed in Chapter 6 can be greatly reduced and better characterized when using a system based on microkelvin, rather than millikelvin temperature calcium atoms. Our success with 3-D QNLC enables us to utilize these ultracold atoms in our ^{40}Ca optical frequency standard. The great

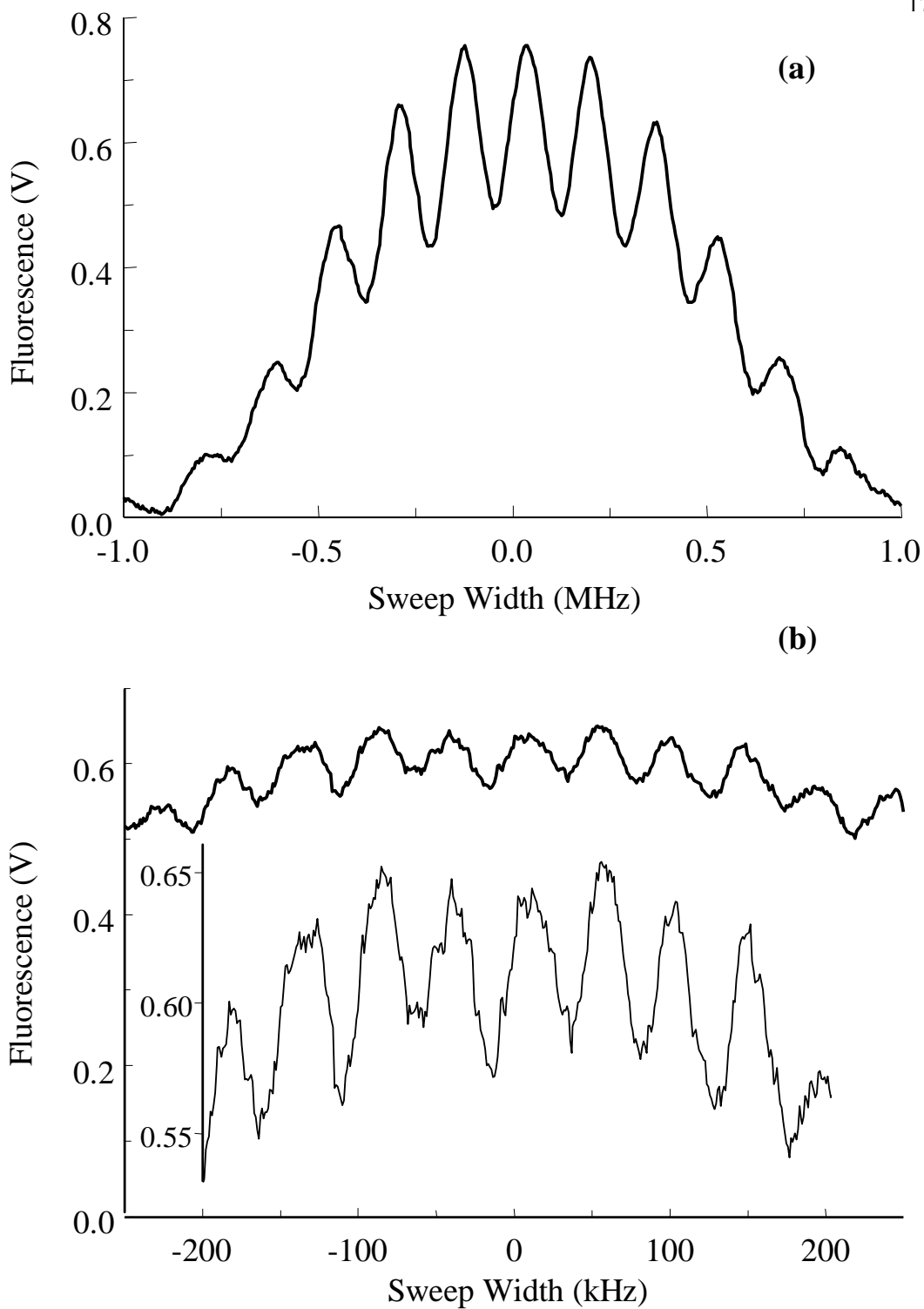


Figure 7.5: Two-pulse Ramsey fringes of an optical transition using ultracold atoms. Trace (a) shows a full sweep of a fringe pattern with a $5 \mu\text{s}$ Ramsey time between the two $\pi/2$ -pulses. Trace (b) is a sweep of only the central fringes created with a $20\text{-}\mu\text{s}$ Ramsey time, shown on an equivalent fluorescence scale as the $T_R = 5 \mu\text{s}$ fringe pattern in order to show the reduction in contrast. The inset is a blow up of the $T_R = 20 \mu\text{s}$ fringe pattern.

reduction in the velocity of the trapped atoms allows better control over and reduction of the drift velocity of the released atom cloud. However, many other systematic effects can also be reduced in this new ultracold system. In this section I begin by discussing how systematic frequency shifts change when using ultracold atoms, then discuss the overall reduction of shifts in our new standard based on ultracold atoms. Important effects include reduced quadratic Zeeman and velocity-related shifts, and methods for better characterization and reduction of shifts due to wavefront curvature and beam overlap.

7.2.1 Systematic effects

7.2.1.1 AC Stark

We now have to worry about an AC-Stark shift due to the 552 nm light that has been added to the system to enable quenched cooling. For our first frequency measurement with ultracold atoms, we calculated a shift of 9 mHz due to the possibility of zeroth-order green light reaching the atoms as leak-through light (measured 18 μW) after the one AOM in the beam path. Recently we moved the shutter AOM to before the fiber on the dye laser table. Only a small percentage of the leak-through light will be coupled through the fiber, further reducing this shift. Additional AOMs have been incorporated into the Ca system to further reduce blue and red leak-through, reducing uncertainties to the millihertz level.

7.2.1.2 Quadratic Zeeman

When using 3-D QNLC, the B-field gradient is reduced from 60 G/cm to 300 mG/cm after the first-stage cooling. Because of the field's small size, we can easily overpower this field by turning on a small bias field in order to make the splittings larger than the Fourier-transform limited width of the velocity distribution, ~ 1 MHz. We set the magnitude of the bias field such that the frequency spacing between $m =$

0 and $m = +1$ or -1 peaks are 2-3 MHz. Recalling that $\Delta\nu = 2.1 \text{ MHz/G}$ for $\Delta m = 1$, this shift corresponds to a field of $\sim 1 \text{ Gauss}$. (We actually fit the $m = +$ or -1 distribution to acquire a value for $\langle B^2 \rangle$.) This field magnitude leads to a frequency shift of 0.6 Hz, which we measure with $< 100 \text{ mHz}$ error.

7.2.1.3 Velocity related effects

If we recall the equations given in Chapter 6 describing the systematic shifts caused in part by the velocity of the atoms, we can see that the frequency shift due to beam overlap goes as the drift velocity, while the shift due to wavefront curvature goes as the v_{rms}^2 of the atom cloud. By using microkelvin atoms, we can effectively reduce this drift velocity from 20 cm/s (on a distribution 70 cm/s wide) to less than 1.5 cm/s (on a distribution 4 cm/s wide). This reduction in drift velocity of a factor of 13 reduces the beam overlap contribution to the error budget by the same factor, to 450 mHz. The reduction of the v_{rms} (70 cm/s \rightarrow 5 cm/s) reduces the effect of the wavefront curvature by a factor of 14^2 to 50 mHz.

At this level, other small velocity dependent terms become non-negligible in the total systematic uncertainty of the system. The largest comes from a term that takes into account the perpendicular offset of the center of the atom cloud from the center of the spectroscopic beams, $r_{0,\perp}$. [88]

$$\Delta\nu = \frac{kv_{rms}r_{0,\perp}}{4\pi} \left(\frac{1}{R_{\uparrow}} + \frac{1}{R_{\downarrow}} \right) \quad (7.3)$$

Due to the 40 m radii of curvature for the beams, R_{\uparrow} and R_{\downarrow} , a $v_{rms} = 5 \text{ cm/s}$, and an uncertainty in the overlap of the atom cloud and the beams of $100 \mu\text{m}$ (for a 1 mm cloud and a 5 mm beam), this shift contributes 190 mHz to the uncertainty of the measurement.

7.2.2 Three-pulse spectroscopy as a diagnostic tool

It is clear from the previous section and the section on systematics in Chapter 6 that increasing the radius of curvature, R , of the spectroscopic beams would reduce shifts further. In principle we can use the atoms themselves as a diagnostic tool combined with the use of different spectroscopic techniques. Multipulse spectroscopy can be configured to be either sensitive to frequency or phase shifts. The spectroscopic sequence of four pulses (the first two pulses incident from the right (\uparrow) and the second two incident from the left (\downarrow)) that we use for our clock spectroscopy can be utilized to measure frequency shifts of the clock transition. A three-pulse spectroscopic sequence with all three pulses coming from the same direction, either $\uparrow\uparrow\uparrow$ or $\downarrow\downarrow\downarrow$, can be used to measure phase shifts, rather than frequency shifts, that occur during the spectroscopic measurement. We can use these different forms of spectroscopy in our system as diagnostic tools for the characterization and reduction of systematic effects.[96]

The phase shift seen in three-pulse Ramsey spectroscopy is given in equation 7.4.

$$\Phi = -\phi_1 + 2\phi_2 - \phi_3 \quad (7.4)$$

Due to the geometry of the system, this phase shift has two terms, one relating to the angle of the spectroscopic beams with gravity and one relating to the radius of curvature as seen in equations 6.24 and 6.27.

$$\Delta\phi(\uparrow\uparrow\uparrow) = (-kg\cos(\alpha_{\uparrow}) - \frac{kv^2}{R_{\uparrow}})T^2 \quad (7.5)$$

and analogously

$$\Delta\phi(\downarrow\downarrow\downarrow) = (-kg\cos(\alpha_{\downarrow}) - \frac{kv^2}{R_{\downarrow}})T^2 \quad (7.6)$$

where k is the wave vector, g is gravity, $\alpha_{\uparrow or \downarrow}$ is the angle between $\vec{k}_{\uparrow or \downarrow}$ and gravity, v is the v_{rms} of the atom cloud, $R_{\uparrow, \downarrow}$ are the radii of curvature for the \uparrow and \downarrow spectroscopic beams, and T is the time between pulses.

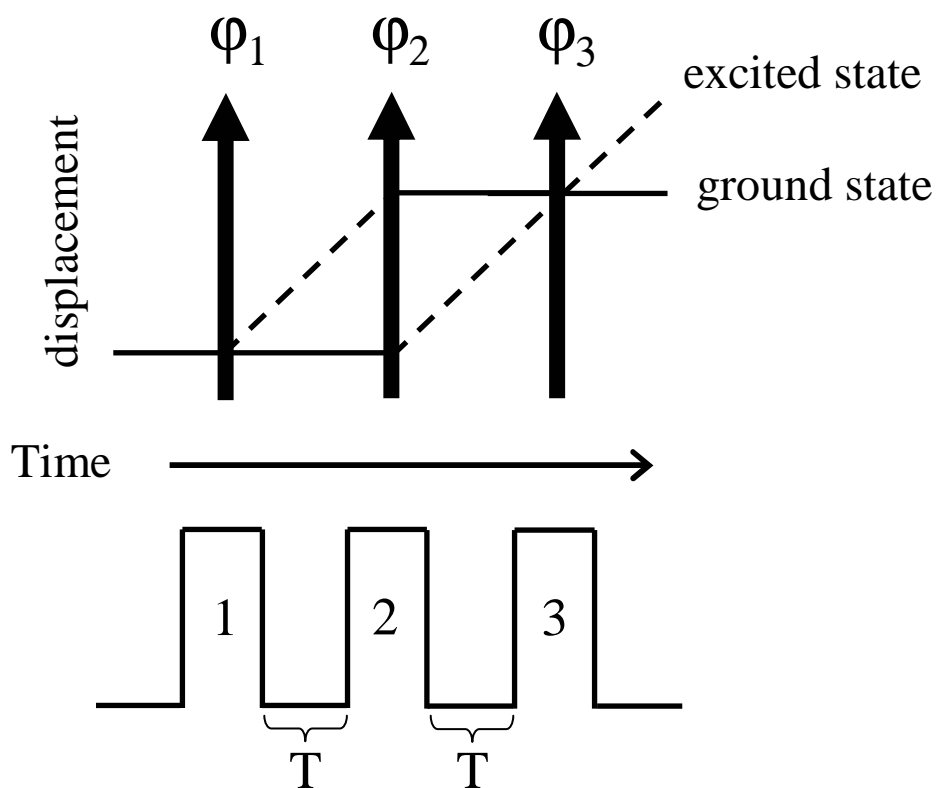


Figure 7.6: Vector and pulse diagram for three-pulse spectroscopy.

While sweeping the phase of the third pulse, one can alternate between a short pulse separation time, T , and a long pulse time and adjust α and R experimentally for both beams to minimize the phase difference between short and long T fringe patterns.[88] This by itself is not enough to prove that both the overlap and radius of curvature shifts have been reduced to zero, as one may not necessarily have cancelled out both individual shifts, but rather made the shifts equal and opposite for this three-pulse spectroscopic detection. Referring to equations 7.5 and 7.6 one can see that to partially uncouple these two systematic effects we can use the fact that only one term (wavefront curvature) is velocity dependent. Instead of comparing the phase of the fringes at different pulses separations, one can observe the phase difference between spectroscopy using fast (3 m/s) and slow (5 cm/s) atoms and adjust the radius of curvature of the beam while performing the three-pulse spectroscopy until there is no phase difference. (Note: with our existing apparatus, this must be done with ultracold atoms as millikelvin atoms travel a significant distance across the magnetic field gradient, causing the Zeeman shift to be coupled with the radius of curvature shift.)

To provide such an increase in the velocity of the atoms we launched them using a -10 MHz detuned 423 nm “pushing” beam. The pushing beams are set incident on the atoms perpendicular either horizontally or vertically to the Bordé-Ramsey spectroscopy beam. (See Figure 7.7 for the effect of horizontal push.) The horizontal pushing beam path is overlapped with the slowing beam path and the vertical pushing beam comes through the top center window of the MOT apparatus. We can impart ~ 3 m/s of velocity in either of these two directions on the ultracold atoms in $\sim 40 \mu\text{s}$, increasing the frequency shift due to wavefront curvature by a factor of 60^2 , as the shift goes as v^2 . With this diagnostic method we should be able to put a new limit of ~ 3 mHz on the possible systematic shifts caused by the wavefront curvature due to this $\propto \frac{v_{rms}^2}{R}$ term, corresponding to a radius of curvature on either beam of $R = 700$ m.

After setting the collimation of the spectroscopy beams, we used the same trick of

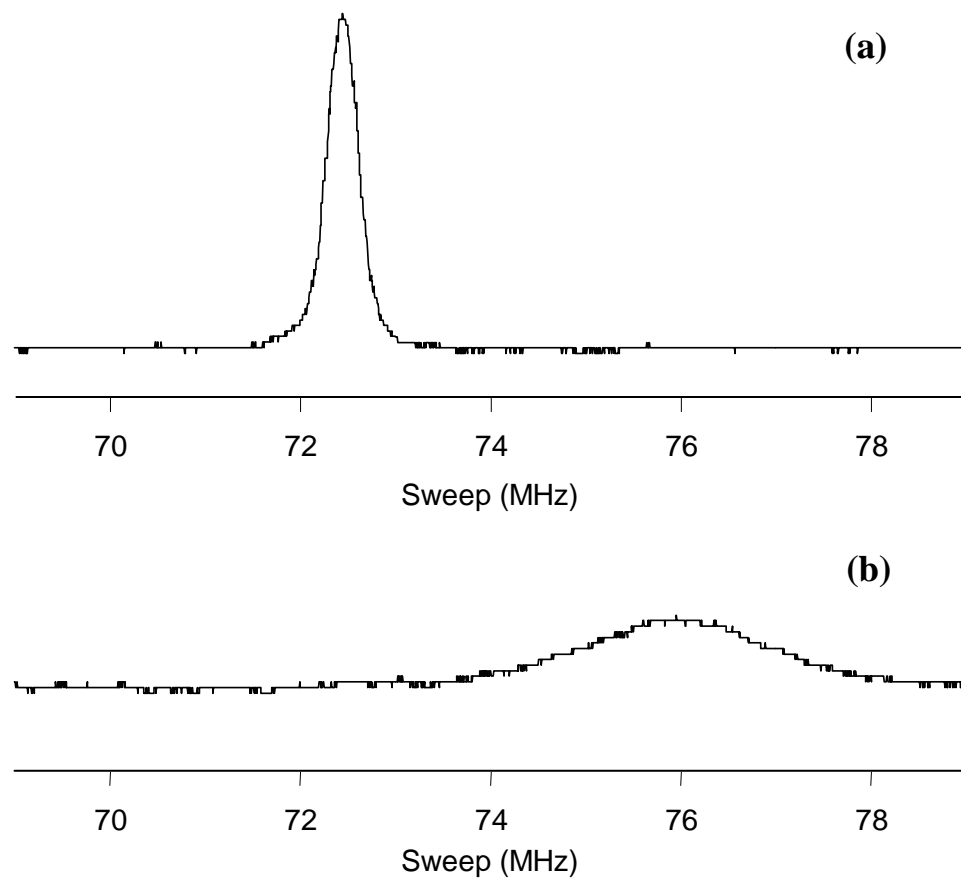


Figure 7.7: To launch the atoms horizontally we turn on the horizontal blue pushing beam for $13 \mu\text{s}$ imparting a velocity of $\sim 1.3 \text{ m/s}$ ($\sim 2 \text{ MHz}$ Doppler shift). Longer pushing times lead to increased launch velocities.

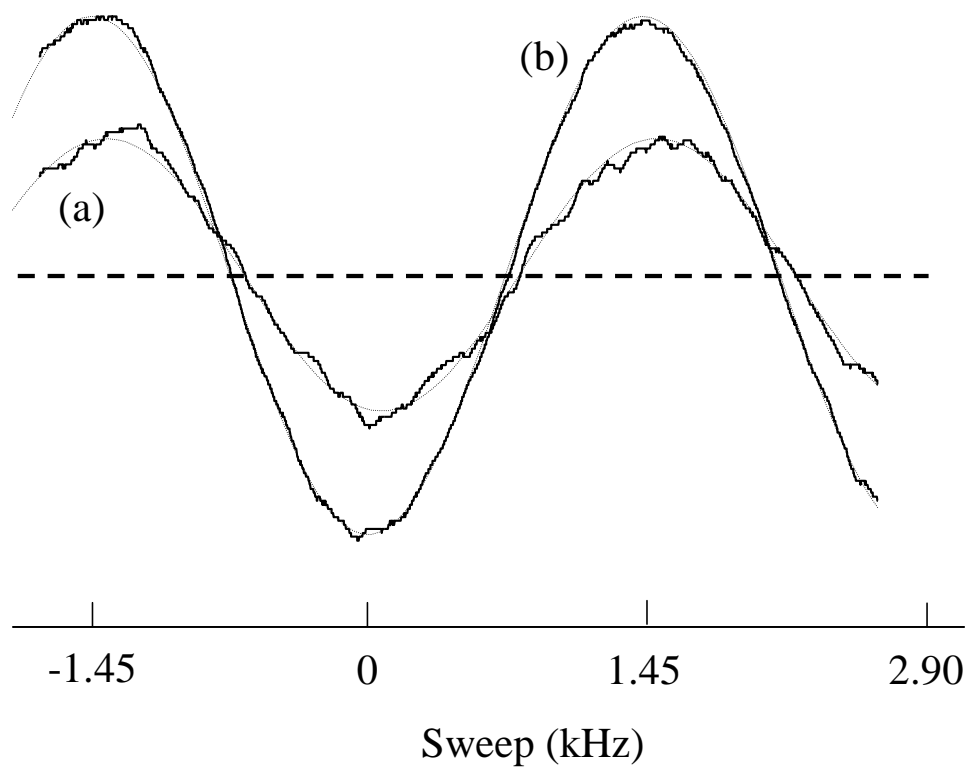


Figure 7.8: We launch the atoms using a blue pushing beam of $30 \mu\text{s}$, imparting a velocity of $\sim 2.4 \text{ m/s}$. We then measure the frequency shift between 1.45 kHz resolution Bordé-Ramsey fringes created while launching the atoms, as shown in trace (a), and fringes made with unpushed atoms, as shown in trace (b). Dotted lines show fits to these two fringe patterns used to measure the frequency shift due to mismatch of beam overlap and this applied transverse velocity.

comparing results from spectroscopy with fast and slow atoms to overlap the beams, this time having utilized four-pulse Bordé-Ramsey spectroscopy and looked for frequency shifts of high resolution (1.45 kHz) fringes when we pushed the atoms transverse to the clock spectroscopy beams. We then overlapped the beams to reduce the frequency shift as much as possible. In Figure 7.8, we compare the Bordé-Ramsey fringe pattern produced with atoms launched to have a drift velocity of 2.4 m/s (trace a) and a fringe pattern created from unpushed atoms (trace b). The two fringe patterns have been fit to Sine functions in order to more accurately measure the frequency shift (dotted lines). The difference was 160 mrad in fringe phase, which at this resolution corresponded to a shift of 74 Hz. As the drift velocity had been increased by a factor of ~ 100 , this corresponds to an uncertainty of only 70 mHz for the frequency error on the clock transition due to beam overlap, which implies an upper limit on the angle between the counterpropagating beams of $6 \mu\text{rad}$.

7.2.3 Summary of systematic effects for microkelvin atoms

Spectroscopic diagnostic methods and ultracold atoms have given us the potential to greatly reduce the overall uncertainty of the ^{40}Ca optical frequency standard. Table 7.1 outlines a new systematic error budget, which includes the new uncertainties derived in this chapter for ultracold atoms, but without the use of three- and four-pulse spectroscopic techniques to reduce velocity dependent shifts (this would reduce the first-order wavefront curvature systematic to a few millihertz and the overlap term to ~ 70 mHz.) The total systematic uncertainty has been reduced to 0.8 Hz, which corresponds to a fractional frequency uncertainty of $< 2 \times 10^{-15}$. The reduction in these systematic uncertainties in a clock based on $10\text{-}\mu\text{K}$ atoms comes from many sources, especially the large reduction in the velocity of the atom cloud, and in the fact that we will increase the resolution of the Bordé-Ramsey spectroscopy from 1.45 kHz to 600 Hz. Many of these uncertainties are also technical in nature and do not set hard limits to the ul-

Table 7.1: Projected systematics budget for the ^{40}Ca optical frequency standard using ultracold atoms ($\sim 10 \mu\text{K}$)

Systematic effect	Correction(Hz)	Uncertainty(Hz)
1st Order Doppler (beam overlap)		0.45
1st Order Doppler (wavefront curvature)		0.25
Locking Errors		0.5
Collision Shift		< 0.25
RF Offsets		< 0.1
AC Stark Shift		0.1
Recoil Overlap		0.25
Blackbody Shift		< 0.1
Quadratic Zeeman shift	~ 1.5	< 0.1
Total:		0.8

mate achievable uncertainty of the Ca optical clock. These include locking errors, the AC-Stark shift and blackbody radiation. Even if these shifts cannot be eliminated (as may be the case for the blackbody shift due to the present vacuum system), it should be possible to quantify and correct for them. The rf offsets may be the most important technological issue. With careful investigation and perhaps the use of three-pulse spectroscopy (after zeroing the gravitational effect) we expect to be able to reduce the uncertainty due to rf offsets by a factor of 10. Collision shifts with microkelvin Ca atoms have not yet been experimentally explored. With millikelvin atoms, we did not see a shift due to atom-atom collisions at the 10 Hz level. Our 10- μK atom cloud has a factor of 10 smaller density, possibly reducing this to < 1 Hz. However, the collision shift may be quite different for microkelvin atoms, as seen in with trapped Cs atoms. If this is the case, we could reduce the density of the atomic cloud, with a trade off in stability, to reduce this shift to the 250 mHz level. This systematic will have to be evaluated more carefully before we can ascribe an experimentally verified uncertainty to this effect.

7.3 Frequency metrology using ultracold atoms

We have made some preliminary measurements of both the stability and the accuracy of the Ca optical frequency standard using microkelvin atoms. Fractional frequency instability measurements made with the femtosecond laser system come in at $1\text{-}2 \times 10^{-14}$ as expected from our own measurements of the S/N of the Bordé-Ramsey fringe. We have also locked the calcium system to high resolution (1.45 kHz) Bordé-Ramsey fringes with ultracold atoms in order to make an absolute frequency measurement. However, we have not yet optimized the launching of the atom cloud and other systematic evaluation techniques that we wish to include in our absolute frequency measurements. When completed these methods should reduce the systematic uncertainty of the Ca optical frequency standard to the 600 mHz level, giving a fractional frequency uncertainty of $\leq 1 \times 10^{-15}$. Presently, we are also preparing for a relative frequency measurement utilizing the Hg^+ optical frequency standard in order to circumvent the limitations of the Cs-based time standard.

In order to reach fractional frequency inaccuracies in the 10^{-16} range, technical improvements must be made to the system. At PTB experiments are in progress to explore the use of calibrated measurement sensors for angle and wavefront curvature systematics, including methods for actively stabilizing the wavefronts of the spectroscopy beams. As velocity related systematics are reduced through the use of three- and four-pulse spectroscopic techniques with launched atoms as I discussed before, other systematic errors at lower levels will surface.

Most technical difficulties can be overcome with diligence and hard work, but large scale improvements enabling uncertainties at the 10^{-17} level will most likely require more drastic changes in the way we trap and manipulate the atoms used to create the clock. In the next section I will discuss a recent development in optical frequency standards of implementing an optical lattice trap for the creation of next-generation optical clocks.

7.4 Lattice trapping

The use of laser cooled and trapped atoms improved the systematic uncertainty of the ^{40}Ca optical frequency standard from $\sim 1\text{-kHz}$ uncertainties possible using thermal atomic beams, to $\sim 10\text{ Hz}$ using millikelvin atoms created in a blue MOT, and to potentially mere Hertz using microkelvin quenched-cooled atoms. The next big step will be the reduction of systematics to the mHz level. In the present experimental setup with ultracold atoms, this level is possible, but technically very difficult. One promising option for large-scale reduction in systematic uncertainty comes from next-generation systems that confine the atoms in an optical lattice, which should allow greater control over perturbations to the trapped atoms and give neutral atoms many of the advantages found previously only in single trapped ions.

The strength of the ion-based optical frequency standards is that the ion itself is held in an extremely non-perturbative manner and cooled so that its motion is confined to $\ll \lambda$ (Lamb-Dicke limit), leading to a smaller overall systematic uncertainty than in neutral-atom-based standards. Unfortunately, the signal-to-noise of a single ion system is significantly less than that of a million-atom system. A multi-atom system can greatly improve the S/N (roughly by a factor a \sqrt{N}), increasing the attainable stability of the frequency standard. Increased short-term stability should allow us to be able to measure fractional frequency inaccuracies at the 10^{-17} level. If an approach can be found to combine the numbers of atoms in neutral-atom traps with the isolation and confinement of an atom in an ion trap, the stability and accuracy of optical clocks could be significantly improved.

In fact, neutral atoms trapped in an optical lattice can fulfill many of these requirements. An optical lattice trap is formed by the intersection of two or more laser beams, or by using a standing wave, which traps atoms in the antinodes of a stable periodic potential of intensity, with a period of $\lambda/2$. Trapping in three-dimensional

optical potential wells was considered as early as 1977 by Letokhov et al. [97] and more recently by Kanzantzev[98], using the AC-Stark shift to confine the atoms in many wells. Also, if the lattice beam is detuned far from resonance, then few photons will be scattered, yielding very low heating rates. We plan to use first- and second-stage cooling to reduce the atom velocity enough to load them into the lattice trap. The lattice beams will then be turned on simultaneously with the MOT beams. Leaving the red and green light on while the lattice loading is taking place will perhaps allow atoms that have slightly more energy than the trap depth to be cooled and trapped during the loading process. Once trapped in a 3-D optical lattice, the atoms are essentially non-interacting, as the density is $\ll 1$ per lattice site.

When using a 1-D lattice, the spacing of the bright and dark fringes in the lattice beam in one dimension creates thin disks of atoms as shown in Figure 7.9. The trap

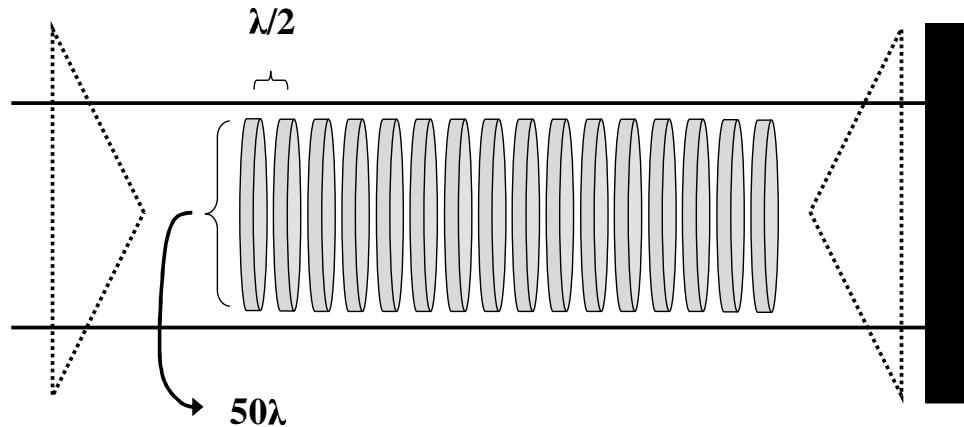


Figure 7.9: A far off resonance 1-D optical lattice for Ca could be formed by making a standing wave out of a focused laser beam at nominally $\lambda = 800$ nm. Atoms only feel a strong trapping force in 1-D and form into discs with a $\lambda/2$ and a width of about 50λ .

depth of an optical lattice is essentially given by the far detuned AC Stark shift (derived originally in chapter 6 see equation 6.11):

$$U_0 \approx \frac{\Omega^2}{4\Delta} \quad (7.7)$$

where Ω is the Rabi frequency and Δ is the detuning of the lattice beams from resonance.

If we assume that the atoms see a harmonic potential ($\frac{1}{2}m\omega^2x_0^2$, valid for microkelvin atoms) at this energy ($\sim U_0$), a beam diameter of 50 μm and a beam power of 500 mW (actually the trapped atoms will see an power four times larger), the lattice trap frequency, $\omega/2\pi$ is ~ 88 kHz parallel to the lattice beam direction due to its tight $\lambda/2$ confinement, and ~ 720 Hz transverse to the beam, due to the 50- μm diameter of the lattice beam. The lattice beam will intersect the red-green MOT in order to load the lattice trap.

Having a strong laser field incident on the atoms during Bordé-Ramsey spectroscopy would normally cause large AC-Stark shifts of the clock transition energy levels, and the lattice trap would need to be turned off during the spectroscopic time, just as the MOT fields must be turned off in our present setup. However, one of the primary advantages of this lattice-trapping scheme is that, for certain frequencies of the lattice beams, the AC-Stark shift created by this light will shift both the ground and excited states equally, leaving the clock transition effectively unshifted, as considered by Katori for Sr.[24] (Note: this “magic wavelength” has been experimentally demonstrated for Sr recently by Ido and Katori in a far off-resonance trap.[99]) If the right lattice frequency can be found for Ca, the lattice can be left on during the Bordé-Ramsey spectroscopy. Preliminary calculations by Chris Oates at NIST show that the wavelength needed for Ca is quite similar to that for Sr calculated by Katori, ~ 800 nm. For ^{40}Ca trapped in a lattice during the spectroscopy, the system gains all the strengths of single-ion standards plus the gain in stability made possible by the S/N of a system of millions of atoms.

A 1-D optical lattice is presently being built for use with our calcium system. A Verdi-pumped titanium-doped sapphire (Ti:Sapph) laser produces the necessary 1 W of 800 nm light. In order to run the laser single frequency and cw, but at the same time avoid power loss due to filtering and tuning devices in the Ti:Sapph cavity, a 780 nm diode laser (20 mW) is used to injection lock the Ti:Sapph laser, as first demonstrated in the group of Scott Bergeson.[100] This diode can then be tuned in an external cavity

and locked to the lattice frequency that correctly cancels the AC-Stark shift between the levels.

Spectroscopy will be performed while the atoms are optically trapped in the lattice. If we hold the atoms in the lattice, there will be no transverse velocity imparted to the atoms by the turning off of the MOT beams, which is presently one of the largest sources of systematic frequency uncertainty. In the lattice configuration, we need only worry about the oscillation frequency of the atoms in the lattice. We can use narrow-line cooling or Raman sideband cooling in order to reach the Lamb-Dicke regime. This should produce an ensemble of atoms on which we can perform recoil- and Doppler-free spectroscopy, as Doppler and recoil shifts are suppressed when atoms are confined to a space much smaller than a wavelength (the Lamb-Dicke limit). In fact, if calcium atoms are trapped in the lattice, cooled to the Lamb-Dicke regime, and then held in the lattice, we could even use two-pulse Ramsey spectroscopy for frequency metrology, increasing the contrast of the fringes and possibly reducing the cycle time.

There are some issues to be dealt with to make the lattice trap an effective method for optical frequency metrology with ^{40}Ca atoms. It is difficult to theoretically derive the correct lattice color for cancelling the shifts to the precision necessary for our frequency standard. Diagnostics performed in a far off-resonance trap (made by focusing the lattice beam to the center of the trap) should make it easier to experimentally determine the correct frequency. We believe that for the best confinement and reduction of systematics we must develop a 3-D lattice trap. Unfortunately, the cancellation of lattice-induced Stark shifts may prove to be extremely difficult for the $^1S_0 \rightarrow ^3P_1$ transition when moving to a 3-D lattice configuration due to polarization considerations (tensor AC-Stark shifts). However, by using odd isotopes and the 3P_0 state, as first pointed out by Katori, [24], there is a single lattice frequency that cancels the frequency shift, even when the lattice beams are configured in three dimensions. In Ca we could use the $^1S_0 \rightarrow ^3P_0$ transition in the ^{43}Ca isotope. This transition is enormously forbidden in the

^{40}Ca isotope, but should have a natural linewidth of on the order of 1 mHz in ^{43}Ca , based on the linewidth of the related transition in Sr. (Recent experiments in Paris have observed and measured the $^1S_0 \rightarrow ^3P_0$ transition frequency in Sr.[101]) With a natural abundance of 0.1 % and commercially available enriched sources, this isotope is a promising choice for a clock, its narrow linewidth increasing the potential fractional frequency instability of the clock system to the $10^{-18}\tau^{-1/2}$. The odd isotope of calcium has another advantage in that it can be cooled using sub-Doppler cooling mechanisms due to its non-zero nuclear spin, removing the added complication of having to use quenched narrow-line cooling to reach microkelvin temperatures. However, if broadband cooling does not allow us to reach $< 10 \mu\text{K}$ temperatures, extra cooling will be needed to efficiently load the lattice.

7.5 Conclusions

Spectroscopic results in ^{40}Ca have been greatly improved with the use of atoms at temperatures less than $10 \mu\text{K}$. These ultracold atoms also cause a large reduction in the systematic uncertainty of the Ca optical frequency standard and the potential for even better stability due to increased contrast and S/N of the Bordé-Ramsey fringes. Atoms that have been cooled using QNLC with reduced 3-D temperatures of $10 \mu\text{K}$ could be loaded into an optical lattice trap, which would give the optical standard the stability of a large N (atom number) system, *and* the achievable accuracy of a single trapped ion. This paradigm shift in the method of confining atoms for frequency metrology is progressing quickly, as groups around the world seek to implement lattice trapping in their alkaline-earth optical frequency standards.